

Northumbria Research Link

Citation: Combrinck, Madeleine (2020) A Note on the Non-Inertial Similarity Solution for Von Kármán Swirling Flow. *Modern Physics Letters B*. ISSN 0217-9849

Published by: World Scientific Publishing

URL: <https://doi.org/10.1142/S0217984921500305>
<<https://doi.org/10.1142/S0217984921500305>>

This version was downloaded from Northumbria Research Link:
<http://nrl.northumbria.ac.uk/id/eprint/43833/>

Northumbria University has developed Northumbria Research Link (NRL) to enable users to access the University's research output. Copyright © and moral rights for items on NRL are retained by the individual author(s) and/or other copyright owners. Single copies of full items can be reproduced, displayed or performed, and given to third parties in any format or medium for personal research or study, educational, or not-for-profit purposes without prior permission or charge, provided the authors, title and full bibliographic details are given, as well as a hyperlink and/or URL to the original metadata page. The content must not be changed in any way. Full items must not be sold commercially in any format or medium without formal permission of the copyright holder. The full policy is available online: <http://nrl.northumbria.ac.uk/policies.html>

This document may differ from the final, published version of the research and has been made available online in accordance with publisher policies. To read and/or cite from the published version of the research, please visit the publisher's website (a subscription may be required.)

A Note on the Non-Inertial Similarity Solution for Von Kármán Swirling Flow

Madeleine L Combrinck

*Department of Mechanical and Construction Engineering, Northumbria University,
Newcastle-upon-Tyne, United Kingdom*

Abstract

This note proposes a non-inertial similarity solution for the classic von Kármán swirling flow as perceived from the rotational frame. The solution is obtained by implementing non-inertial similarity parameters in the non-inertial boundary layer equations. This reduces the partial differential equations to a set of ordinary differential equations that is solved through an integration routine and shooting method.

Keywords: incompressible, constant rotation, derivation, boundary layer.

1. Introduction

Flow over a rotating disk is a classic example in fluid mechanics. It is a simplified representation for systems that comprise of rotating components where incompressible flow and constant, pure rotation can be assumed. An approximation to the solution was first proposed by von Kármán [1] with a more rigorous calculation provided by Cochran [2]. The solution process was described by Schlichting [3] using the boundary layer equations in cylindrical

*Corresponding author

Email address: `madeleine.combrinck@northumbria.ac.uk` (Madeleine L Combrinck)

co-ordinates:

$$\begin{aligned}
\frac{\partial u_r}{\partial r} + \frac{u_r}{r} + \frac{1}{r} \frac{\partial u_\theta}{\partial \theta} + \frac{\partial u_z}{\partial z} &= 0 \\
u_r \frac{\partial u_r}{\partial r} + \frac{u_\theta}{r} \frac{\partial u_r}{\partial \theta} - \frac{u_\theta^2}{r} + u_z \frac{\partial u_r}{\partial z} &= -\frac{\partial \psi}{\partial r} + \nu \frac{\partial^2 u_r}{\partial z^2} \\
u_r \frac{\partial u_\theta}{\partial r} + \frac{u_\theta}{r} \frac{\partial u_\theta}{\partial \theta} + \frac{u_\theta u_r}{r} + u_z \frac{\partial u_\theta}{\partial z} &= -\frac{1}{r} \frac{\partial \psi}{\partial \theta} + \nu \frac{\partial^2 u_\theta}{\partial z^2}
\end{aligned} \tag{1}$$

A non-dimensional parameter, η , is introduced which is a function of the perpendicular wall distance and the square root of the rotational velocity and the kinematic viscosity. This is a stretching parameter that represents the non-dimensional wall distance in the perpendicular direction.

$$\eta = z \sqrt{\frac{\omega}{\nu}} \tag{2}$$

The family of partial derivatives related to Equation 2 are not generally reported in literature. These will be used in later derivation by substituting in Equation set 1.

$$\begin{aligned}
\frac{\partial}{\partial \eta} &= \frac{\partial}{\partial z} \sqrt{\frac{\nu}{\omega}} \\
\frac{\partial^2}{\partial^2 \eta} &= \frac{\partial^2}{\partial z^2} \frac{\nu}{\omega}
\end{aligned} \tag{3}$$

Further parameters, that render the velocity components and pressure non-dimensional, is proposed [3] in a manner where $F(\eta)$ becomes the non-dimensional velocity in the radial directions. Similarly, $G(\eta)$ and $H(\eta)$ represent the non-dimensional velocities in the tangential and axial directions respectively.

$$\begin{aligned}
u_r &= r\omega F(\eta) \\
u_\theta &= r\omega G(\eta) \\
u_z &= \sqrt{\nu\omega} H(\eta) \\
p &= p_0 + \rho\nu\omega P(\eta) \\
\psi &= \frac{p}{\rho}
\end{aligned} \tag{4}$$

The parameters above are selected in a manner that will not only render the
10 boundary layer equations non-dimensional upon substitution, but also transform the partial differential equations into ordinary differential equations. The

stretching parameter η is obtained using the Buckingham π theorem of dimensional analysis [4, 5]. Using dimensional analysis further, the dimensionless form of the velocity and pressure parameters are obtained by dividing them by
 15 constant reference properties such as the free stream tangential velocity ($r\omega$), kinematic viscosity (ν), density (ρ), and pressure (p_0) [6, 7].

Equations 2, 3 and 4 are substituted into Equation set 1. This leads to a set of non-dimensional boundary layer equations [3]. (From this point in the paper the η term is neglected from the notation to facilitate easier reading and understanding.)

$$\begin{aligned}
 2F + H' &= 0 \\
 F^2 + F'H - G^2 - F'' &= 0 \\
 2FG + HG' - G'' &= 0
 \end{aligned}
 \tag{5}$$

The equations above represent a two-point boundary value problem that can be resolved with integration methods (i.e. 2nd order Euler or 4th order Runge Kutta methods) to determine the values at each distance step. This is coupled
 20 with a shooting method (i.e. bisection or Newton's methods) to determine the values of the higher order derivatives at the wall, $F'(0)$ and $G'(0)$. The result from this operation is shown in Figure 1.

2. Rationale

The von Kármán solution is presented in the inertial frame; therefore, the
 25 Centrifugal and Coriolis accelerations are not present in the momentum equation. Understanding the nature of an inertial frame versus a non-inertial frame, and it's application in fluid dynamics, is notoriously problematic. It is best explained at the hand of an example using the perspective of an observer. Imagine that there is an observer standing on a train platform looking at an incoming
 30 train. From the perspective of the observer the train is in motion while the surrounding landscape is stationary. In the event where the train accelerates or decelerates the resulting forces will not act on the observer. In contrast to

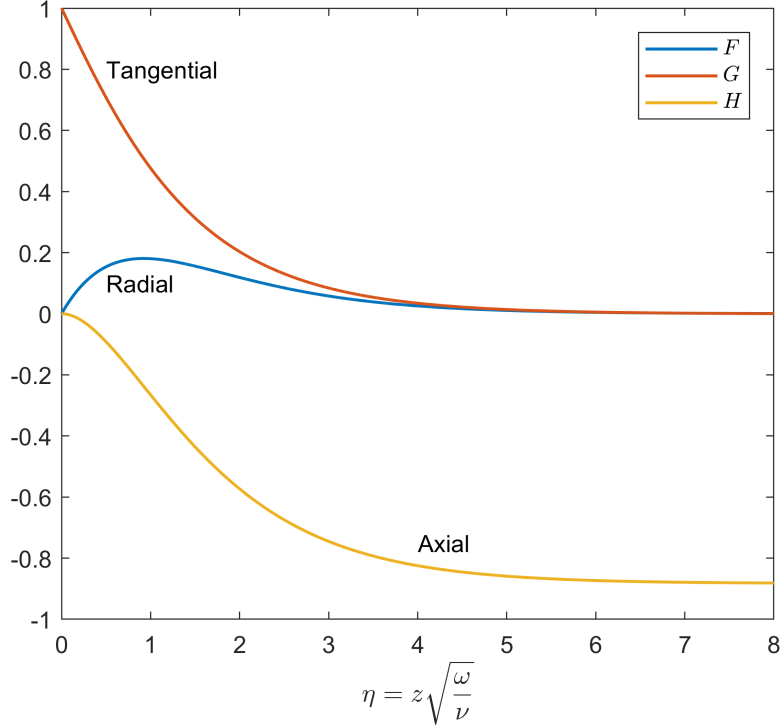


Figure 1: Inertial Solution to the von Karman Rotating Disk (Equation 5), as a function of η

this, now perceive the train from the perspective of a passenger on the train. From their point of view, the train is stationary and the landscape is passing by as if it is in motion. During acceleration and deceleration the resulting forces will act on the observer in this frame of reference. The forces resulting from the relative motion of the train is referred to as fictitious forces that can only be quantified from the non-inertial frame. Considering rotating systems from a non-inertial perspective allows for further understanding of the physical mechanisms that are responsible for flow features. The fictitious forces, such as the Centrifugal and Coriolis terms, are explicitly defined and the effect thereof can be determined directly (Figure 2).

In the inertial frame, the far-field flow is stationary, while the disk is in motion. The boundary layer is formed in the near-wall region. The tangential

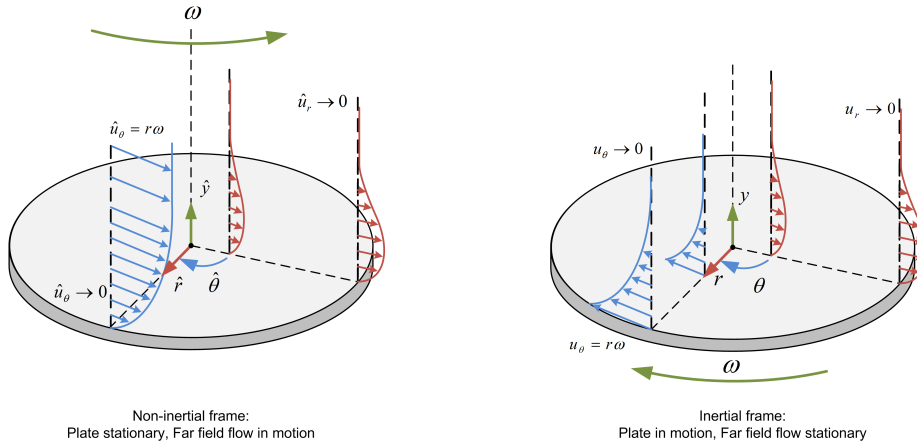


Figure 2: Flow over a rotating plate interpreted from the non-inertial frame (left) and the inertial frame (right) [8]

velocity profile therefore has a high velocity just above the disk (nearly the same velocity as the disk), and approaches stationary conditions in the far-field. This flow can also be observed from a non-inertial theoretical framework. From this perspective, the disk is stationary and the far-field flow is in rotation. This flow rotation in the non-inertial frame has the same rotational velocity as the rotating disk in the inertial frame. The gradient of the tangential velocity in the boundary layer is consistent between the two frames. Considering the non-dimensional velocity profiles, the value of G on the wall will be 1 and approach 0 in the far-field. The value for \hat{G} , the superscript $\hat{\cdot}$ indicating vectors in the non-inertial frame, will be 0 on the wall and 1 in the far-field. Assuming that the velocity gradient is the same between the two frames, the following non-dimensional relation should hold:

$$G = 1 - \hat{G} \quad (6)$$

The radial and axial velocities should be equal between the two frames. In both cases the radial flow is forced outwards from the centre of rotation as a result of the disk motion and the flow rotation respectively. This causes the axial flow in both cases to flow in the direction towards the plate. The resulting equations

should hold for this analogy to be correct:

$$\begin{aligned} F &= \hat{F} \\ H &= \hat{H} \end{aligned} \tag{7}$$

This paper is aimed at deriving a non-inertial solution to the von Kármán swirling flow problem. The solution obtained should adhere to the assumptions stated in Equations 6 and 7. These conditions will serve as validation for any possible solution.

The von Kármán similarity solution has been expanded to problems with heat transfer [9, 10], non-Newtonian flows [11, 12], magnetohydrodynamic flows [13, 14] and flow over stretching disks [15, 16, 17]. In these cases the parameter η , along with the other non-dimensional parameters ($F(\eta), G(\eta), H(\eta)$), is uniquely defined to ensure that a non-dimensional, ordinary differential equation set is obtained. η can be similar to the original definition of von Kármán in some cases (Equation 2), but not in general. The ideal set of non-dimensional parameters need to be obtained for a substitution that is relevant to the flow under investigation. Following the Buckingham π theory to obtain the form of η will not lead to a unique definition for η ; there will be numerous solutions or π groups. There are a multitude of options available since the only requirement is that η remains non-dimensional and is not dependant on density in incompressible flow. The correct π grouping, representing the definition of η , must be implemented. It was rightly noted in [6] that solutions are based on prior knowledge and benefit from previous experience for the form of η . That brings the question for this current problem: Can the non-dimensional parameters of the inertial frame of the von Kármán similarity solution be used to derive a solution in the non-inertial frame?

3. Mathematical Model

The non-inertial boundary layer equations for a rotating disk in incompressible and pure rotation were derived using an Eulerian method by [8]. Using these equations (Equations 8, 10 and 12) and substituting the non-inertial

forms of Equations 2, 3 and 4 provides a set of non-dimensional equations in
70 the non-inertial frame (Equations 9, 11 and 13).

The conservation of mass equation in cylindrical co-ordinates is given as follows:

$$\frac{\partial \hat{u}_r}{\partial \hat{r}} + \frac{\hat{u}_r}{\hat{r}} + \frac{1}{\hat{r}} \frac{\partial \hat{u}_\theta}{\partial \hat{\theta}} + \frac{\partial \hat{u}_z}{\partial \hat{z}} = 0 \quad (8)$$

Substitution, as shown in the previous section, and simplification lead to the following expression:

$$\begin{aligned} \frac{\partial}{\partial \hat{r}} \hat{r} \hat{\omega} \hat{F} + \frac{1}{\hat{r}} \hat{r} \hat{\omega} \hat{F} + \frac{1}{\hat{r}} \frac{\partial}{\partial \hat{\eta}} \hat{r} \hat{\omega} \hat{G} + \frac{\partial}{\partial \hat{\eta}} \sqrt{\frac{\hat{\omega}}{\hat{\nu}}} \sqrt{\hat{\nu} \hat{\omega}} \hat{H} &= 0 \\ \hat{\omega} \hat{F} + \hat{\omega} \hat{F} + \hat{\omega} \hat{H}' &= 0 \\ 2\hat{F} + \hat{H}' &= 0 \end{aligned} \quad (9)$$

The radial momentum equations,

$$\hat{u}_r \frac{\partial \hat{u}_r}{\partial \hat{r}} + \frac{\hat{u}_\theta}{\hat{r}} \frac{\partial \hat{u}_r}{\partial \hat{\theta}} - \frac{\hat{u}_\theta^2}{\hat{r}} + \hat{u}_z \frac{\partial \hat{u}_r}{\partial \hat{z}} = -\frac{\partial \hat{\psi}}{\partial \hat{r}} + \hat{\nu} \frac{\partial^2 \hat{u}_r}{\partial \hat{z}^2} - \underbrace{2\hat{u}_\theta \hat{\omega}}_{\text{Coriolis}} + \underbrace{\hat{r} \hat{\omega}^2}_{\text{Centrifugal}} \quad (10)$$

is reduced as a similar manner:

$$\begin{aligned} \hat{r} \hat{\omega} \hat{F} \frac{\partial}{\partial \hat{r}} \hat{r} \hat{\omega} \hat{F} + \frac{\hat{r} \hat{\omega} \hat{G}}{\hat{r}} \frac{\partial}{\partial \hat{\theta}} \hat{r} \hat{\omega} \hat{F} - \frac{1}{\hat{r}} (\hat{r} \hat{\omega} \hat{G})^2 + \sqrt{\hat{\nu} \hat{\omega}} \hat{H} \frac{\partial}{\partial \hat{\eta}} \sqrt{\frac{\hat{\omega}}{\hat{\nu}}} \hat{r} \hat{\omega} \hat{F} &= -\frac{\partial}{\partial \hat{r}} \left(\frac{\hat{p}}{\hat{\rho}} + \hat{\nu} \hat{\omega} \hat{p} \right) \\ + \hat{\nu} \frac{\partial^2}{\partial \hat{\eta}^2} \frac{\hat{\omega}}{\hat{\nu}} \hat{r} \hat{\omega} \hat{F} - 2\hat{r} \hat{\omega} \hat{G} \hat{\omega} + \hat{r} \hat{\omega}^2 & \\ \hat{r} \hat{\omega}^2 \hat{F}^2 - \hat{r} \hat{\omega}^2 \hat{G}^2 + \hat{r} \hat{\omega}^2 \hat{H} \hat{F}' = \hat{r} \hat{\omega}^2 \hat{F}'' - 2\hat{r} \hat{\omega}^2 \hat{G} + \hat{r} \hat{\omega}^2 & \\ \hat{F}^2 - \hat{G}^2 + \hat{H} \hat{F}' - \hat{F}'' + 2\hat{G} - 1 = 0 & \end{aligned} \quad (11)$$

This procedure is also followed in the reduction of the tangential momentum equation,

$$\hat{u}_r \frac{\partial \hat{u}_\theta}{\partial \hat{r}} + \frac{\hat{u}_\theta}{\hat{r}} \frac{\partial \hat{u}_\theta}{\partial \hat{\theta}} + \frac{\hat{u}_\theta \hat{u}_r}{\hat{r}} + \hat{u}_z \frac{\partial \hat{u}_\theta}{\partial \hat{z}} = -\frac{1}{\hat{r}} \frac{\partial \hat{\psi}}{\partial \hat{\theta}} + \hat{\nu} \frac{\partial^2 \hat{u}_\theta}{\partial \hat{z}^2} + \underbrace{2\hat{u}_r \hat{\omega}}_{\text{Coriolis}} \quad (12)$$

leading to a non-dimensional relationship.

$$\begin{aligned}
\hat{r}\hat{\omega}\hat{F}\frac{\partial}{\partial\hat{r}}\hat{r}\hat{\omega}\hat{G} + \frac{\hat{r}\hat{\omega}\hat{G}}{\hat{r}}\frac{\partial}{\partial\hat{\theta}}\hat{r}\hat{\omega}\hat{G} + \frac{\hat{r}\hat{\omega}\hat{G}\hat{r}\hat{\omega}\hat{F}}{\hat{r}} + \sqrt{\hat{\nu}\hat{\omega}}\hat{H}\frac{\partial}{\partial\hat{\eta}}\sqrt{\frac{\hat{\omega}}{\hat{\nu}}}\hat{r}\hat{\omega}\hat{G} &= -\frac{1}{\hat{r}}\frac{\partial}{\partial\hat{\theta}}\left(\frac{\hat{p}}{\hat{\rho}} + \hat{\nu}\hat{\omega}\hat{p}\right) \\
&+ \hat{\nu}\frac{\partial^2}{\partial\hat{\eta}^2}\frac{\hat{\omega}}{\hat{\nu}}\hat{r}\hat{\omega}\hat{G} + 2\hat{r}\hat{\omega}\hat{F}\hat{\omega} \\
\hat{r}\hat{\omega}^2\hat{F}\hat{G} + \hat{r}\hat{\omega}^2\hat{F}\hat{G} + \hat{r}\hat{\omega}^2\hat{H}\hat{G}' &= \hat{r}\hat{\omega}^2\hat{G}'' + 2\hat{r}\hat{\omega}^2\hat{F} \\
2\hat{F}\hat{G} + \hat{H}\hat{G}' - \hat{G}'' - 2\hat{F} &= 0
\end{aligned} \tag{13}$$

The derivation results in a set of non-dimensional partial differential equations in the non-inertial frame:

$$\begin{aligned}
2\hat{F} + \hat{H}' &= 0 \\
\hat{F}^2 - \hat{G}^2 + \hat{H}\hat{F}' - \hat{F}'' + 2\hat{G} - 1 &= 0 \\
2\hat{F}\hat{G} + \hat{H}\hat{G}' - \hat{G}'' - 2\hat{F} &= 0
\end{aligned} \tag{14}$$

The fictitious forces were simplified in a manner where the resulting equations are functions of the non-dimensional velocity parameters \hat{G}, \hat{F} and \hat{H} . These ordinary differential equations were resolved using a 2nd order Euler integration method coupled with Newton's shooting method to resolve the boundary layer profile. This is known as a two-point boundary value problem. The numerical methods in MATLAB used here are described in [18, 19].

80 4. Results

The original solution of von Karman (Equation 5) requires boundary conditions to be resolved [3]. The radial velocity (F) is zero both at the wall and in the far-field. The tangential velocity is normalised using the wall velocity, which means that the condition at the wall is equal to one and zero in the far-field:

$$\begin{aligned}
\eta = 0 : F = 0, G = 1, \\
\eta = \infty : F = 0, G = 0
\end{aligned} \tag{15}$$

The following equivalent boundary conditions in the non-inertial field, considering that in this frame the flow is rotating and plate is stationary, is proposed:

$$\begin{aligned}\eta = 0 : \hat{F} = 0, \hat{G} = 0, \\ \eta = \infty : \hat{F} = 0, \hat{G} = 1\end{aligned}\tag{16}$$

Additional boundary values are required to obtain a solution. While $F(0)$, $G(0)$ and $H(0)$ are known, the additional values needed for the beginning value problem, $F'(0)$ and $G'(0)$ are unknown. Using the knowledge that $F(\infty) = 0$ and $G(\infty) = 0$, a shooting method can be employed to resolve the boundary layer flow as shown in Figure 1. The beginning values for $F'(0)$ and $G'(0)$ are hence determined:

$$\begin{aligned}\eta = 0 : F' = 0.51023, G' = -0.61592, H = 0 \\ \eta = \infty : F' = 0, G' = 0, H = -0.88446\end{aligned}\tag{17}$$

In the inertial frame, the non-dimensional tangential velocity starts at a value of one at the wall and decreases monotonically to reach zero in the far-field. The profile in the non-inertial frame starts at zero and increases monotonically to reach a value of one in the far-field. The tangent of both profiles will therefore be equal but of opposite sign, as reflected in the beginning values below. The remainder of the beginning values for the non-inertial frame are inferred using the analogies of Equations 6 and 7:

$$\begin{aligned}\eta = 0 : \hat{F}' = 0.51023, \hat{G}' = 0.61592, \hat{H} = 0 \\ \eta = \infty : \hat{F}' = 0, \hat{G}' = 0, \hat{H} = -0.88446\end{aligned}\tag{18}$$

Solving the equation set 14 as a two-point boundary value problem with an integration method results in the solution depicted in Figure 3. The significance of the result is shown in Figure 4 where the solutions between the inertial and the non-inertial frames are compared at using the analogies of Equations 6 and 7. It is observed that the assumptions of Equations 6 and 7 holds true, therefore validating the solution in the non-inertial frame.

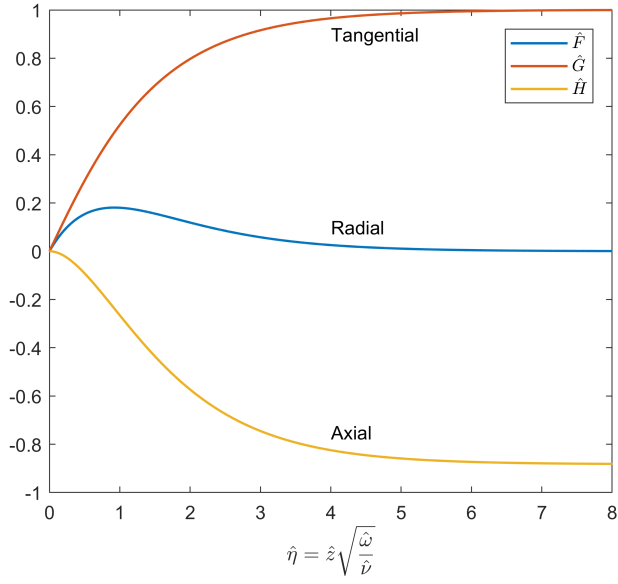


Figure 3: Non-inertial Solution to the von Kármán Rotating Disk (Equation 14)

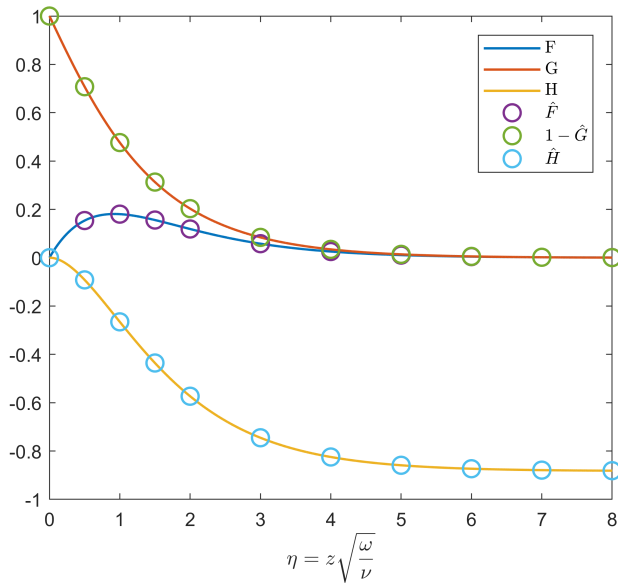


Figure 4: Comparison between the Inertial and Non-inertial Solutions of the Rotating Disk

Exact solutions to the Navier-Stokes equations are used to gain a deeper understanding flow features in the boundary layer. Along with solutions such
90 as the Blasius boundary layer problem [20] and Stokes boundary layer problem [3], the von Kármán solution falls in this category. It can be studied in the original form or under various conditions such as heat transfer, non-Newtonian flow, magnetohydrodynamics flow and flow with partial slip. Exact solutions also serve as benchmark cases to validate numerical methods implemented in
95 Computational Fluid Dynamic (CFD) codes. Here the author established an exact solution for the swirling flow problem from a non-inertial frame of reference which have not been seen in this form in open literature to date. Results from a CFD solver that is written specifically to operate in the non-inertial frame [21] can be directly compared with the non-inertial solution of the von Kármán
100 problem. With the inclusion of the fictitious forces, this solution paves the way to establish exact solutions for more complex problems in the non-inertial frame. An example of this is rotating objects in axial flow where six fictitious forces act on the object in unsteady conditions [22].

5. Conclusions

105 This work on swirling flow has shown the potential of the non-inertial model:

- The non-inertial similarity solution to the von Kármán swirling flow problem proposed here, can be used to directly validate numerical simulation results for rotational cases.
- The technical note established the framework for obtaining similarity so-
110 lutions of more complex flow problems in non-inertial frames.

References

- [1] T. von Karman, Uber laminare und turbulente reibung, *Z. Angew. Math. Mech.* 1 (1921) 233–252.
- [2] W. G. Cochran, The flow due to a rotating disc, *Mathematical Proceedings of the Cambridge Philosophical Society* 30 (3) (1934) 365–375.
115
- [3] H. Schlichting, *Boundary-Layer Theory*, 3rd Edition, McGraw-Hill, 1968.
- [4] E. Buckingham, On physically similar systems; illustrations of the use of dimensional equations, *Physical Review* 4 (4) (1914) 345–376.
- [5] E. Buckingham, The principle of similtude, *Nature* 96 (2406) (1915) 396–397.
120
- [6] P. Childs, *Rotating Flow*, 1st Edition, Elsevier Inc., 2011.
- [7] H. P. Greenspan, *The Theory of Rotating Fluids*, 1st Edition, Cambridge University Press, 1968.
- [8] M. Combrinck, L. Dala, I. Lipatov, Eulerian derivation of non-inertial navier–stokes and boundary layer equations for incompressible flow in constant pure rotation, *European Journal of Mechanics - B/Fluids* 65 (2017) 10 – 30.
125
- [9] C. Soong, C. Chyuan, Similarity solutions of mixed convection heat and mass transfer in combined stagnation and toation-induced flows over a rotating disk, *Heat and Mass Transfer* 34 (1998) 171–180.
130
- [10] A. Kendoush, Similarity solution for heat convection from a porous rotating disk in a flow field, *ASME Journal of Heat Transfer* 135 (8) (2013) 084505.
- [11] H. Andersson, E. de Korte, R. Meland, Flow of a power-law fluid ove a rotating disk revisited, *Fluid Dynamic Research* 28 (2001) 75–88.

- 135 [12] H. Andersson, M. Rousselet, Swirling flow of bingham fluids above a rotating disk: An exact solution, *Journal of Non-Newtonian Fluid Mechanics* 197 (2006) 329–335.
- [13] M. Turkyilmazoglu, Mhd fluid flow and heat transfer due to a stretching rotating disk, *International Journal of Thermal Sciences* 51 (2012) 195–201.
- 140 [14] M. Mustafa, Mhd nanofluid flow over a rotating disk with partial slip effect: Buongiorno model, *International Journal of Heat and Mass Transfer* 108 (B) (2017) 1910–2016.
- [15] A. Hobiny, B. Ahmad, A. Alsaedi, M. Jalil, S. Asghar, Similarity solution for flow over an unsteady nonlinearly stretching rotating disk, *AIP Advances* 5 (047133) (2015) 396–397.
- 145 [16] C. Wang, Review of similarity stretching exact solutions of the navier-stokes equations, *European Journal of Mechanics - B/Fluids* 30 (5) (2011) 475–479.
- [17] H. Andersson, M. Rousselet, Slip flow over a lubricated rotating disk, *International Journal of Heat and Fluid Flow* 27 (2) (2006) 329–335.
- 150 [18] L. Zheng, X. Zhang, Chapter 8 - numerical methods, in: L. Zheng, X. Zhang (Eds.), *Modeling and Analysis of Modern Fluid Problems*, Mathematics in Science and Engineering, Academic Press, 2017, pp. 361 – 455.
- [19] G. Lindfield, J. Penny, Chapter 6 - boundary value problems, in: G. Lindfield, J. Penny (Eds.), *Numerical Methods (Fourth Edition)*, fourth edition Edition, Academic Press, 2019, pp. 301 – 328.
- 155 [20] H. Blasius, Grenzschichten in Flüssigkeiten mit kleiner Reibung, *Z. Angew. Math. Phys.* 56 (1908) 1–37.
- [21] M. L. Combrinck, Boundary Layer Response to Arbitrary Accelerating Flow, Ph.D. thesis, University of Pretoria (2017).
- 160

- [22] M. Combrinck, L. Dala, I. Lipatov, Non-Inertial Forces in Aero-Ballistic Flow and Boundary Layer Equations, R&D Journal of the South African Institution of Mechanical Engineering 33 (2017) 85–96.

Declaration of Interest Statement

165 The author declares that she has no conflict of interest.

Nomenclature

Super Scripts and Sub Scripts

$\hat{}$	Rotational frame
r	r-direction
170 θ	θ -direction
z	z-direction

Alphabet

p	Pressure
t	Time
175 u	Velocity
r	Distance in r-direction
z	Distance in z-direction
F	Non-dimensional parameter
G	Non-dimensional parameter
180 H	Non-dimensional parameter

Greek Letters

η	Dimensionless wall distance
ν	Kinematic viscosity
ρ	Density
185 ψ	Pressure per unit mass
ω	Rotational velocity